Carbohydrate Polymers 229 (2020) 115534

Contents lists available at ScienceDirect

Carbohydrate Polymers

journal homepage: www.elsevier.com/locate/carbpol

Urinary metabolomics analysis reveals the anti-diabetic effect of stachyose in high-fat diet/streptozotocin-induced type 2 diabetic rats

Li Liang[a,b], Guimei Liu[c], Guoyong Yu[a,b], Fuming Zhang[d], Robert J. Linhardt[d], Quanhong Li[a,b,*]

[a] Beijing Advanced Innovation Center for Food Nutrition and Human Health, College of Food Science and Nutritional Engineering, China Agricultural University, Beijing 100083, China
[b] National Engineering Research Center for Fruit and Vegetable Processing, Beijing 100083, China
[c] School of Food Sciences and Engineering, Qilu University of Technology, Jinan 250353, China
[d] Departments of Chemical and Biological Engineering, Chemistry and Chemical Biology, Biomedical Engineering and Biological Science, Center for Biotechnology and Interdisciplinary Studies, Rensselaer Polytechnic Institute, Troy, NY 12180, USA

ARTICLE INFO

Keywords:
Stachyose
Metabolomics
Type 2 diabetes
Rats
UPLC-ESI-Q-TOF-MS

ABSTRACT

As a new platform of systems biology, metabolomics provides a powerful approach to discover therapeutic biomarkers and mechanism of metabolic disease. Type 2 diabetes mellitus (T2DM) is a global metabolic disease, thus, a urinary metabolomics profiling was analyzed to study the anti-diabetic effects and mechanism of stachyose (ST) on high-fat diet- and low dose streptozotocinc-induced T2DM rats. The results showed that ST treatment regulated the level of insulin, low-density lipoprotein cholesterol, and triglycerides, which demonstrates improvement in T2DM on ST treatment. Urinary samples from the ST and T2DM group were enrolled in metabolomics study, 21 differential metabolites were identified from urinary metabolomics analysis, indicating that the ST treatment partly exerted the anti-diabetes activity by regulating energy metabolism, gut microbiota changes and inflammation. A metabolomics strategy is both suitable and reliable for exploring the anti-diabetes effects and understanding the mechanisms of ST treatment against T2DM.

1. Introduction

Type 2 diabetes mellitus (T2DM) is a metabolic disorder characterized by chronic hyperglycemia with disturbances of carbohydrate, fat and protein metabolism arising out of defects in insulin secretion and/or insulin action (Schwarz et al., 2013). The global prevalence of T2DM has continuously increased and was estimated at 2.8% in 2000 and 4.4% in 2030 (Wild, Roglic, Green, Sicree, & King, 2004). The development of T2DM results from hereditary, environmental and nutritional factors, and it is highly correlated with the uptake of a high-fat diet (Schwarz et al., 2013). Chronic hyperglycemia inherently leads to downstream metabolic dysfunction including imbalance of carbohydrate, fat and protein metabolism and hyperlipidemia in relevant organs and blood plasma. Therefore, metabolic changes are central to these disorders, and powerful analytical approaches are required to detect metabolism biomarkers during the development and treatment of T2DM (Faber et al., 2007).

Metabolomics is a cross-disciplinary discipline downstream from the genome, transcriptome, and proteome (Nicholson, Lindon, & Holmes, 1999). It provides an approach to comprehensively profile the low-molecular-weight molecules (metabolites) in a living system (Nicholson et al., 1999). Metabolomics has developed rapidly and demonstrated enormous potential in many fields, such as disease diagnosis, medical research, food nutrition research and other areas in human health care (Dunn & Ellis, 2005). The application of metabolomics technologies in the study of T2DM have been used and some biomarkers are involved in pathogenesis and response to therapy in T2DM (Guasch-Ferré et al., 2016).

Stachyose (ST), is a water-soluble tetrasaccharide extracted from *Rehmanniae radix*, a traditional Chinese medicine. ST can significantly decrease the blood glucose level in hyperglycemic rats (Zhang et al., 2004). ST, composed of one glucose, one fructose and two galactoses units, is naturally occurring in many vegetables and plants (Yin, Yang, Wang, & Chen, 2006). The mechanism for the anti-diabetic effect of ST

Abbreviations: T2DM, type 2 diabetes mellitus; MT, metformin; ST, stachyose; HFD, high-fat diet; STZ, streptozotocin; NH_4F, ammonium fluoride; FA, formic acid; WG, weight gain; Ins, insulin; Glu, blood glucose; TC, total cholesterol; TG, triglyceride; TP, total protein; ALT, alanine aminotransferase; QC, quality control; PCA, principal component analysis; OPLS-DA, orthogonal partial least squares discriminant analysis; VIP, variable influence on projection; RT, retention time; EMA, ethylmalonic acid

* Corresponding author at: College of Food Science and Nutritional Engineering, China Agricultural University, Beijing 100083, China.
E-mail address: quanhong_li@hotmail.com (Q. Li).

https://doi.org/10.1016/j.carbpol.2019.115534
Received 11 April 2019; Received in revised form 28 September 2019; Accepted 24 October 2019
Available online 31 October 2019
0144-8617/

on T2DM rats remains unclear. In recent years, ultra-performance liquid chromatography-mass spectrometry (UPLC-MS) has become recognized as a powerful platform in metabolomics studies. The analytical system has the advantages of high sensitivity, specificity, rapid analysis and reproducibility, particularly in the global determination of low-molecular weight metabolites in biological samples (Wang et al., 2012). In our current study, we undertook urinary metabolomics analysis to investigate the metabolic profiles and differential metabolites in the rat model of T2DM. After treatment of T2DM rats with ST, using UPLC quadrupole time-of-flight mass spectrometry (Q-TOF)-MS. This study aimed to discover the effects of ST on different metabolic pathways and the mechanisms of anti-diabetic effects of ST in T2DM rats.

2. Materials and methods

2.1. Materials

Stachyose with a purity of ~80% was purchased from Xi'an Feide Biotech Co., Ltd. (Xi'an, China). Streptozotocin (STZ), ammonium acetate (NH_4Ac), ammonium hydroxide (NH_4OH), ammonium fluoride (NH_4F), and formic acid (FA) were purchased from Sigma (St. Louis, MO, USA). Acetonitrile was purchased from Merck (Darmstadt, Germany). Rat insulin ELISA Kit was obtained from Mercodia AB (Uppsala, Sweden).

2.2. Animal experiments

Adult male Wistar rats (weighing 200 ± 20 g) were supplied by Beijing Laboratory Animal Research Center (Beijing, China). The experimental protocols for current studies were approved by the Ethics Committee of Beijing Laboratory Animal Research Center (SYXK2015-0046; Beijing, China). 40 rats were housed in SPF barrier environment with standard environmental conditions of the constant temperature of 21–23 ℃, relative humidity of 40%–45%, and 12 h light (6:00 a.m.) /dark (6:00 p.m.) cycle with *ad libitum* access to food and water. After a week of acclimatization, 10 rats randomly allocated to control group, which were continually fed on a normal diet and intragastrically administered with saline after 4 weeks. Meanwhile, 30 rats were fed on a high-fat diet (HFD), consisting of 10% lard, 20% sucrose, 2.5% cholesterol, 1% sodium cholate and 66.5% pulverized standard rat pellet (Liu et al., 2018). After 4 weeks of HFD feeding, the rats were intraperitoneally injected once with low-dose of STZ (30 mg/kg body weight). The T2DM rat model was established successfully as indicated as the fasting blood glucose level ≥11.1 mmol/L and the presence of polyuria and polydipsia (Mayyas, Alzoubi, & Bonyan, 2016). The T2DM rat models were randomly assigned to three groups with 10 rats in each: (1) T2DM group, continually feed with HFD diet and intragastrically administered with saline; (2) ST treatment group (ST group), fed with HFD diet and intragastrically administered with 5000 mg/kg body weight of stachyose once daily; (3) Metformin treatment group (MT group), fed with HFD diet and intragastrically administered with 200 mg/kg body weight metformin once daily (Dong, Chen, Yang, Shou, & Li, 2016). Two rats in T2DM and one in MT group died during the experiment. Fasting glucose levels and body weight gain (WG) was monitored at baseline and throughout the study

2.3. Samples collection and preparation

To collect urine samples, all the rats from each group were hosted in metabolic cages (1 rat per cage). Urine samples were collected from individual metabolic cages rats for 24 h. Then, samples were centrifuged at 8000 rpm at 4 ˚C for 15 min. The supernatants were immediately frozen in liquid nitrogen, and then stored at −80 ˚C until analysis. Samples were thawed on ice before analysis. Urine sample (50 μL) was mixed with 200 μL of MeOH (−20 ˚C), mixed by vortex (30 s) and incubated for 2 h at −20 ˚C to precipitate proteins, which were then removed by centrifugation at 13,000 rpm for 15 min. The supernatant was filtered through a 0.22 μm membrane filter before UPLC-MS analysis.

Blood samples were collected through ocular sampling for isolating serum (centrifuged at 12,000 × g, 10 min, 4℃). Blood glucose (Glu), total cholesterol (TC), triglyceride (TG), high-density lipoprotein cholesterol (HDL), low-density lipoprotein cholesterol (LDL) and other blood biochemical parameters, such as total protein (TP), and alanine aminotransferase (ALT), were measured by a fully automatic biochemical analyzer (Hitachi, Japan) in the Health Science Center of Peking University (Pecking, China) as previously described (Zhang, Xu, Yu, Yi, & Sui, 2017). Insulin (Ins) was determined by an ELISA kit according to the manufacturer's instructions.

2.4. LC–MS/MS analysis (HILIC/MS)

Urinary metabolomics profiling was analyzed using a UPLC-ESI-Q-TOF-MS system (UHPLC, 1290 Infinity LC, Agilent Technologies, Santa Clara, CA, USA) coupled to a quadrupole time-of-flight (AB Sciex TripleTOF 6600, Framingham, MA, USA).

For hydrophilic interaction liquid chromatography (HILIC) separation, samples were analyzed using a 2.1 mm × 100 mm ACQUIY UPLC BEH 1.7 μm column (Waters, Ireland). The flow rate was 0.5 mL/min and the mobile phase contained: A = 25 mM ammonium acetate and 25 mM ammonium hydroxide in water and B = acetonitrile (ACN). The gradient was 85% B for 1 min and was linearly reduced to 65% in 11 min, and then reduced to 40% in 0.1 min and maintained for 4 min, and then increased to 85% in 0.1 min, with 5 min re-equilibration period employed. Both electrospray ionization (ESI) positive-mode and negative mode were applied for MS data acquisition. The ESI source conditions were set as follows: Ion Source Gas 1 as 60, Ion Source Gas 2 as 60, curtain gas as 30, source temperature: 600 ˚C, IonSpray Voltage Floating (ISVF) ± 5500 V. In MS only acquisition, the instrument was set to acquire over the *m/z* range 60–1000 Da, and the accumulation time for TOF MS scanning was set at 0.20 s/spectra. In auto MS/MS acquisition, the instrument was set to acquire over the *m/z* range 25–1000 Da, and the accumulation time for production scan was set at 0.05 s/spectra. The product-ion scan was acquired using information dependent acquisition with high sensitivity mode selected. The collisional energy was fixed at 35 V with ± 15 eV. Declustering potential was set as ± 60 V.

The samples were randomly analyzed by UHPLC-QTOF-MS. Quality control (QC) samples were prepared by pooling aliquots of all samples that were representative of the urine samples under analysis and used for data normalization. Blank samples (75%ACN in water) and QC samples were injected every five samples during acquisition.

2.5. Multivariate data processing and data analysis

The separated metabolites were ionized with ESI positive and negative mode, respectively. The raw data were converted into mzML format using the ProteoWizard software, and then the XCMS program was used to calibrate the retention-time, extract peak-integration and normalization of the data from different eight-plexes. The identity of each ion was searched against the house database ((Shanghai Applied Protein Technology Co., Ltd.) for molecular annotation.

In the extracted-ion features, only the variables having more than 50% of the nonzero measurement values in at least one group were kept (Smith, Want, O'Maille, Abagyan, & Siuzdak, 2006). For the multivariate statistical analysis, the MetaboAnalyst (www.metaboanalyst.ca) web-based system was used. After the Pareto scaling, principal component analysis (PCA) was performed. Statistical analysis was performed using multivariate statistics combined with univariate statistics. Normalized data were exported to SIMCA-P + (Version 12.0, Umetrics, Sweden) to perform orthogonal partial least squares discriminant analysis (OPLS-DA) and a model was built to identify variables that

accounted for the differentiation of T2DM group and ST group. The leave one out cross-validation and response permutation testing were used to evaluate the robustness of the model. The significant different metabolites were determined based on the combination of a statistically significant threshold of variable influence on projection (VIP) values obtained from OPLS-DA model and two-tailed Student's *t*-test (*p* value) on the raw data, and the metabolites with VIP values larger than 1.0 and *p* values less than 0.1 were considered as differential metabolites.

The basic significance statistics were performed by one-way analysis of variance with SPSS 17.0 Version (SPSS Inc., Chicago, IL, USA). Differences with a $p < 0.05$ were considered significant. Data is shown as mean ± standard deviations (SD).

2.6. Differential metabolites identification and pathway analysis

Metabolic and reconstruction of pathway metabolites of interest were extracted from OPLS-DA score plots based on their contribution to the variation and correlation within the data set. Concerning the identification of differential metabolites, the ion spectra were matched with the structural message of metabolites acquired from biochemical databases, such as HMDB, http:// www.hmdb.ca/; Mass-Bank, http:// www.massbank.jp/ and KEGG, http:// www.genome.jp/kegg/. The reconstruction pathway analysis was performed with MetPA software (http://metpa.metabolomics.ca) based on the above database sources to identify the metabolic pathways.

3. Results and discussion

3.1. Anti-diabetic effects of ST in T2DM rats

Table 1 shows the body WG, insulin and blood serum parameters determined by biochemical analysis. When compared with the T2DM group and Control group, both ST and MT groups showed decreases in TP concentration ($p < 0.05$) after four weeks of treatment. In addition, ST treatment significantly reduced the level of Ins, LDL-c, TG and ALT ($p < 0.05$). There's no significant differences in TC ($p = 0.07$), HDL-c ($p = 0.42$) among the three groups. These results were consistent with previous reports indicated that ST treatment showed the improvement of insulin resistance and hypolipidemic effects on T2DM rats (Liu et al., 2018; Poovitha, Sai, & Parani, 2017). The mean body WG and Glu of ST group were improved when compared with T2DM group and control group, but the differences were not statistically significant.

3.2. Urine metabolic profiling by UHPLC-Q-TOF/MS

A quality control (QC) sample was tested in every five samples using both positive-ion mode (ESI+) and negative-ion mode (ESI-) ESI detection to validate the reliability of the system. Total ion chromatography (TIC) spectra of QC samples were overlayed and compared. The results suggested that the response intensity and retention time of the QCs overlapped, indicating that this method was robust and showed good stability and low variation caused by the instrumental error. Typical metabolites spectra of the urine samples obtained by LC–MS are shown in Fig. 1. The peaks well separated from one another, indicating that the chromatographic and MS conditions were suitable for the measurement of the samples in this study.

Data integrity and accuracy are preconditions for statistical and biological significance, but metabolite concentrations often span several orders of magnitude, leading to misidentification of significant changes. Thus, it was essential to first check the data integrity, deleting missing values and extreme values, then normalizing the data between samples and metabolites to reduce any systematic bias or technical variation. In the extracted-ion features, the metabolites having more than 50% missing measurement values were not used in subsequent analysis.

The overall distribution trend among all samples can be observed using PCA analysis, and possible discrete points can be identified. PCA score plots are presented in Fig. 2. The total variance in the data represented by the first two principal components in the positive-ion mode was 46.4% (Fig. 2A). In the negative-ion mode, the first two principal components could represent 45.9% of the total variance in the data (Fig. 2B). There was a slight, but not significant, separation trend in the PCA score plots between the two groups.

OPLS-DA was subsequently performed in consideration of the void supervision of the PCA model to further construct and discriminate the differential metabolites between groups. Using this approach distinct separated clusters were observed between the metabolite profiles of two groups (Fig. 3A). The parameters of the OPLS-DA model (R2Y, Q2) were obtained by 7-fold cross-validation both in the positive-ion mode (R2Y = 1.000, Q2 = 0.686) and negative ion mode (R2 = 0.997, Q2 = 0.578) to evaluate the fitness and the prediction ability of our model (Neth et al., 2015). The R2Y and Q2 were ≥ 0.5, suggesting the model was stable and reliable. The permutation test of the OPLS-DA model built on the positive-ion and negative-ion mode are shown in Fig. 3B. Overfitting did not occur in the OPLS-DA model in the present experiment.

From all the PCA and OPLS-DA score plots, we can see clear separation trends in both positive-ion and negative-ion modes, indicating that the urinary metabolic profiles were different at baseline between ST and T2DM groups. The urine metabolic profiling analysis is supported by the biochemical parameters, both demonstrating the anti-diabetic effects of ST treatment on T2DM rats. It can also be speculated that the anti-diabetic mechanism of ST is related to changes in levels of a few metabolites.

3.3. Detection and identification of differential metabolites

Based on the VIP values, the expression pattern of each metabolite in the affecting intensity and explanatory ability was measured so potential metabolites could be discovered. In our study, differentially expressed metabolites were selected according to the parameter VIP > 1 and *P* value < 0.05 (significant differential metabolites) or

Table 1
The effects of ST and MT groups on blood biochemical parameters.

Group	T2DM	MT	ST	Control	P value
Body WG (g)	−5.56 ± 21.58 a	1.00 ± 15.29 a	14.88 ± 23.84 a	54.32 ± 19.86 b	0.508
Ins (μIU/mL)	45.20 ± 3.57 a	46.01 ± 8.12 a	35.70 ± 2.53 b	11.19 ± 2.49 c	< 0.05
Glu (mmol /L)	34.16 ± 6.99 a	21.34 ± 7.02 b	30.66 ± 2.29 ab	8.72 ± 1.44 c	0.421
TG (mmol /L)	1.73 ± 0.56 a	1.08 ± 0.71 ab	0.74 ± 0.39 bc	0.45 ± 0.19 c	< 0.05
TC (mmol /L)	5.67 ± 2.23 a	3.07 ± 1.04 a	3.89 ± 1.78 a	1.62 ± 0.30 b	0.076
LDL (mmol /L)	2.93 ± 2.17 a	1.32 ± 0.81ab	0.84 ± 0.33 bc	0.25 ± 0.08 d	< 0.05
HDL (mmol /L)	1.22 ± 0.35	1.08 ± 0.26	1.14 ± 0.22	1.30 ± 0.22	0.425
TP (g/L)	61.32 ± 3.77 a	53.84 ± 4.06 b	54.76 ± 2.16 b	63.9 ± 3.8 a	< 0.05
ALT (U/L)	122.13 ± 8.25 a	123.80 ± 19.28 a	83.97 ± 24.07 b	47.30 ± 9.32 c	< 0.05

Data are presented as mean ± SD. Values in the same row with different letters (a–c) are significantly different, $p < 0.05$.

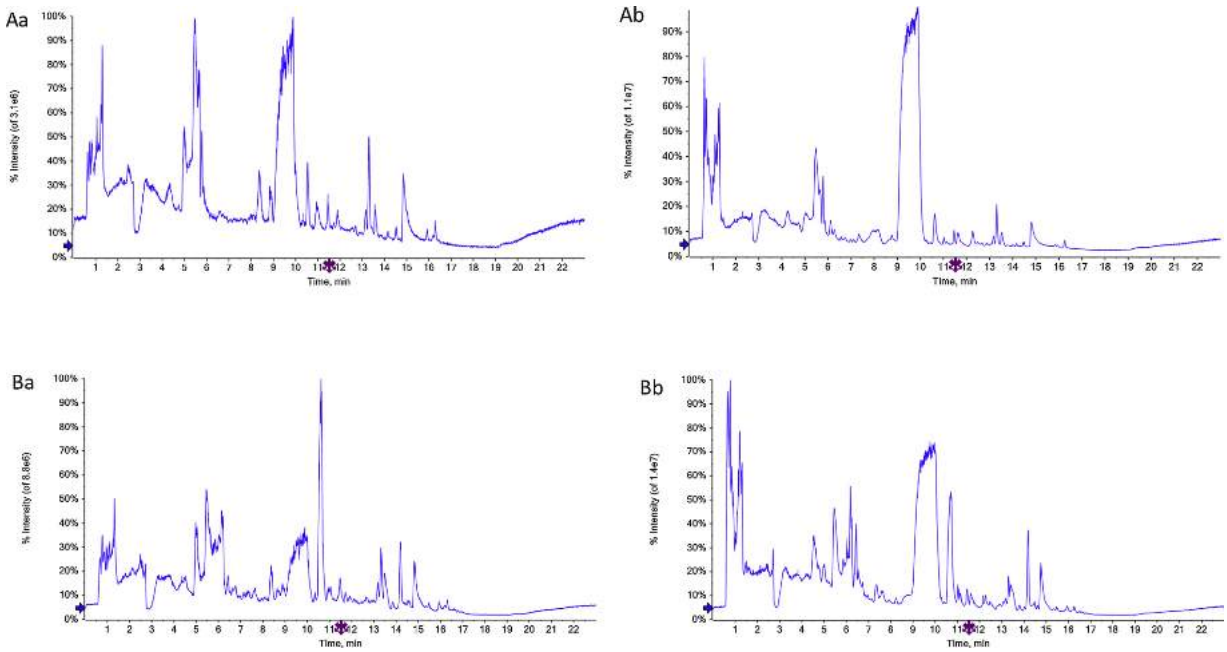

Fig. 1. Representative UHPLC-QTOF/MS total ion chromatograms (TIC) of urine obtained from the T2DM groups (A) and ST groups (B) analyzed in positive (a) and negative (b) modes, respectively.

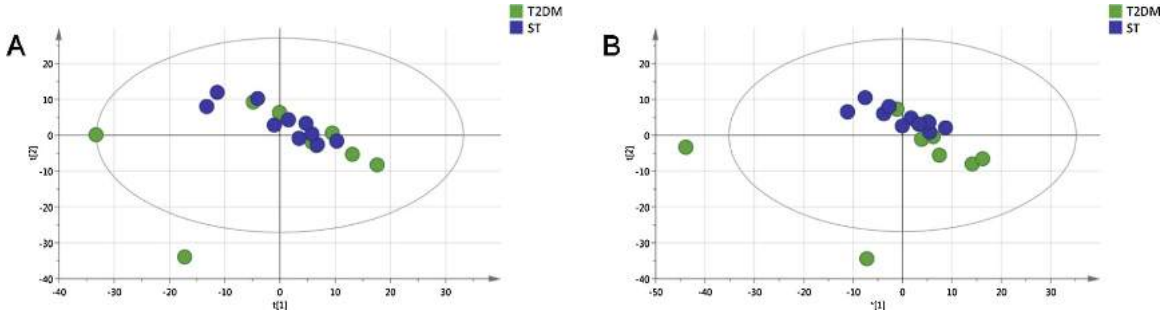

Fig. 2. PCA analysis in positive (A) and negative (B) mode of the ST vs T2DM, respectively.

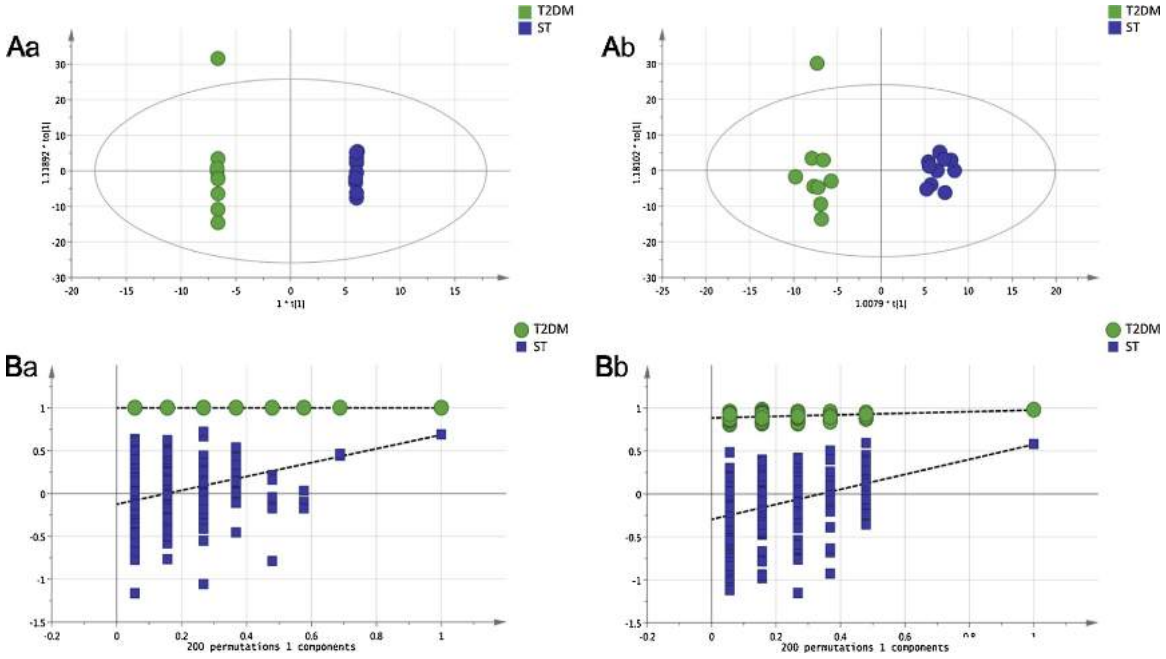

Fig. 3. OPLS-DA analysis (A) and OPLS-DA permutation test (B) in positive (a) and negative (b) mode of the ST vs T2DM, respectively.

Table 2
Identification results of differential metabolites in between T2DM and ST groups in urine.

Mode	Metabolite No.	Adduct	RT (s)	m/z	Metabolite	VIP	Fold change	*P* value
ESI (+)	1	(M+H)+	530.24	220.12	Pantothenate	2.14	1.87	0.0030
	2	(M+H)+	271.15	139.05	Nicotinamide N-oxide	4.69	3.06	0.012
	3	(M+H)+	116.70	104.07	3-Aminobutanoic acid	2.47	2.15	0.012
	4	(M + NH4)+	844.12	192.05	trans-Aconitic acid	1.11	1.74	0.023
	5	(M+H-H2O)+	692.21	143.12	N6-Methyl-L-lysine	6.57	2.58	0.025
	6	(M+H)+	73.61	169.07	beta-Carboline	1.43	2.32	0.027
	7	(M + NH4)+	244.07	196.08	L-Gulonic gamma-lactone	1.31	1.49	0.028
	8	(M+H)+	843.94	175.02	cis-Aconitate	1.04	1.56	0.033
	9	(M+H)+	886.85	193.03	Citrate	2.29	1.74	0.059
	10	(M+H)+	428.16	153.07	Ribitol	1.12	3.71	0.078
	11	(M+H)+	682.88	112.09	Histamine	1.02	0.56	0.080
	12	(M+H)+	616.00	126.10	1-Methylhistamine	3.41	0.61	0.090
ESI (-)	13	(M-H)-	752.02	174.04	N-Acetyl-aspartic acid	1.70	2.32	0.00019
	14	(M-H)-	271.43	165.06	3-Hydroxyphenyl propanoic acid	13.55	2.51	0.00093
	15	(M-H)-	770.97	133.01	L-Malic acid	4.89	1.92	0.0015
	16	(M-H)-	243.83	177.04	L-Gulonic gamma-lactone	3.01	1.74	0.0028
	17	(M-H)-	698.55	145.01	Alpha-ketoglutarate	7.53	1.56	0.0057
	18	(M + CH3COO)-	154.50	207.09	Mevalonic acid	1.25	3.35	0.0092
	19	(M-H)-	121.55	153.02	Gentisic acid	2.89	2.15	0.020
	20	(M-H)-	880.32	191.02	Citrate	9.87	1.97	0.031
	21	(M-H)-	626.86	131.03	Ethylmalonic acid	1.24	0.27	0.038
	22	(M-H)-	317.60	163.04	4-Hydroxycinnamic acid	1.31	1.85	0.041
	23	(M-H)-	839.08	129.02	Citraconic acid	2.13	1.46	0.049
	24	(M-H)-	857.36	173.01	cis-Aconitate	1.29	1.40	0.076

VIP > 1 and 0.05 < *P* value < 0.1 (differential metabolites). Several potential urinary metabolites were identified by comparing the retention time (RT) and mass spectra of authentic standards as well as the standard MS/MS spectra from the above databases. The compound name, RT, measured *m/z*, VIP values, P-values, and FC of each differentially expressed metabolite under the positive-ion and negative-ion mode of ST compared to T2DM groups are provided in Table 2.

Taking the two ESI detection modes into consideration, 21 compounds were selected as the differential metabolites between the two groups, and 17 of them were significant differential metabolites in urine. Furthermore, among the differential metabolites observed, the expression of 10/11 metabolites was up-regulated for the ESI+/ESI-in ST compared to T2DM, and that of 2/1 was down-regulated for the ESI+/ESI-. VIP score of the metabolites was positively associated with the influence on the separation of sample classification, thus, metabolites with VIP score ranking at the top are noteworthy. In the ESI + mode, metabolites of nicotinamide *N*-oxide, pantothenate, maltotriose, 3-aminobutanoic acid, histamine and 1-methylhistamine appear to be the key metabolites for anti-diabetic effect based on their VIP score and results of previous studies. Likewise, metabolites of *N*-acetyl-aspartic acid, 3-hydroxyphenyl propanoic acid, citrate, alpha-ketoglutarate, and ethylmalonic acid are identified in the ESI- mode.

Hierarchical clustering analysis is a common method in data mining and statistics. Cluster 3.0 software was applied to further depict the specific and unique expression patterns of these differentially expressed metabolites in the urine of T2DM and ST treated rats. Java TreeView software was used to generate heatmaps (Fig. 4), which shows a global overview of all the urinary metabolites that were detected and visualized. As shown in the heatmaps and dendrogram, metabolites with similar variation trends in abundance were positioned closer together, suggesting that the close clustering of the ST treated metabolites and their separation from the T2DM group.

3.4. KEGG pathway enrichment analysis

The KEGG online database was applied to pathway enrichment analysis, which explores the most relevant pathways and the potential mechanisms. The Fisher' exact method was used to calculate the significance of the enriched pathways. Pathway enrichment analysis identified all matched pathways based on *p* values and pathway rich factors from pathway topology analysis. In general, the smaller the p value is, the more significant the enrichment is. The magnitude of the enrichment factor indicates the reliability of significance. As shown in Fig. 5, results suggested that citrate cycle (TCA cycle), alanine, aspartate and glutamate metabolism, glyoxylate and dicarboxylate metabolism and glucagon signaling pathway were mainly influenced pathways of ST therapy in urine.

3.5. Biochemical interpretation

Combined with previous studies, the differential metabolites connected with carbohydrate, fatty acid and gut microbiota metabolism, which related to the pathogenesis of T2DM, revealed the intervention effect of ST on T2DM.

The TCA cycle is a crucial metabolic pathway that occurs in the inner mitochondrial membrane and connects various anabolic and catabolic biochemical pathways which modulate the electron transport chains, ultimately resulting in the production of energy by generating ATP. The final products of fatty acid degradation and glycolysis are included in the TCA cycle, and TCA cycle intermediates are involved in amino acid synthesis and degradation. As shown in a non-targeted metabolomics study, a reduction in the mitochondrial TCA cycle was associated with the development of diabetes (Oexle, Gnaiger, & Weiss, 1999). Citrate, α-ketoglutarate, malic acid and cis-Aconitate are main intermediates in TCA cycle. Previous studies demonstrated that urinary citrate, malate and alpha-ketoglutarate were significantly decreased in diet-induced hyperlipidemia and diabetes (Azam et al., 2017; Liu et al., 2012). In the current study, the level of citrate, malic acid and α-ketoglutarate in the ST treated rat urine samples were found to be increased considerably as compared with T2DM groups, probably implying that ST treatment affected the T2DM by improving energy metabolism. In addition, an absolute or relative deficiency of insulin plays a primary role in the metabolic disorders linked to diabetes, leading to liver glycolysis and glycogen synthesis decrease. Citrate is a source of NAD + required for the glycolytic pathway. In the liver, citrate serves as a regulator of glycolysis and gluconeogenesis by satisfying NAD + required for the glycolytic pathway, thus, can regulate blood glucose levels. It also provides acetyl-CoA in the synthesis of fatty acids. The coupling of glycolytic NADH production with the mitochondrial electron transport chain, such as malate–aspartate shuttle,

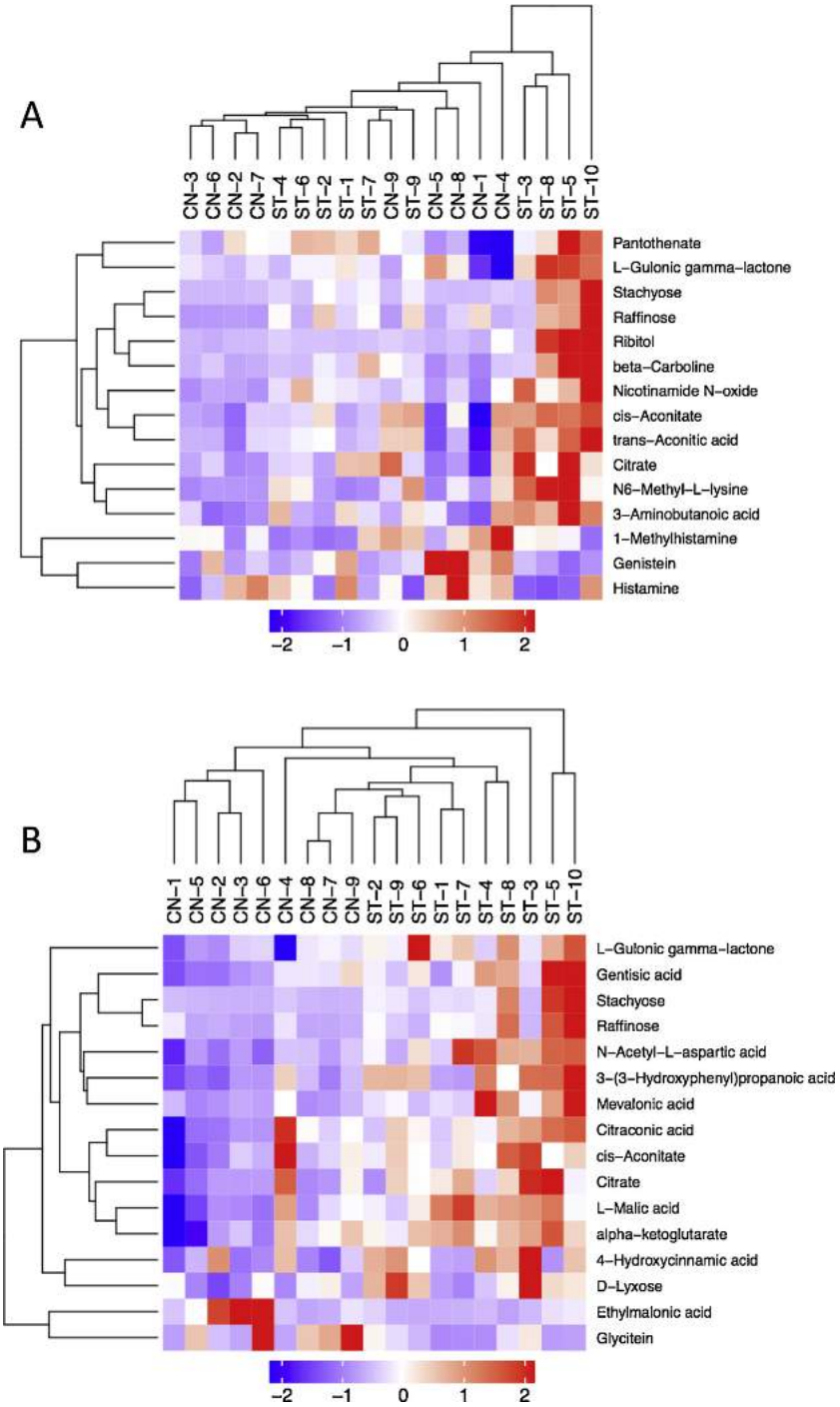

Fig. 4. Hierarchical clustering representation of the differentially expressed metabolites profiles in positive (A) and negative (B) mode of the ST vs T2DM, respectively.

is crucial for pancreatic β-cell function and energy metabolism. Accordingly, increased levels of intermediates in TCA cycle demonstrate that ST treatment modulates mitochondrial function by increasing the TCA cycle activity.

In human urine, organic acids provide information on energy production, intestinal bacterial action, fatty acid, carbohydrate and protein metabolism. The obvious increase of acidic metabolites in urine samples of ST group, such as 3-aminobutanoic acid and 3-hydroxyphenyl propanoic acid, is associated with the gut microbiota metabolism. As many studies report, the gut microbiome is closely related to the pathogenesis of T2DM and conspires to perturb metabolic homeostasis and health together with genetic susceptibility and environmental factors (Napolitano et al., 2014; Shin et al., 2014). Thus, the gastrointestinal tract is an important target for functional natural products. Hydroxyphenyl propanoic (HMPP) acid is the metabolite of anaerobic bacteria, such as *Clostridia* and *Bacaeroides*. Moreover, research has suggested the decreased trends of *Clostridia* among T2DM patients (Larsen et al., 2010). HMPP is suspected of physiological effects through the prevention of antioxidant stress (Hold, Schwiertz, Aminov, Blaut, & Flint, 2003). 3-Aminobutanoic acid, also known as beta-aminobutyric acid, can be biosynthesized from butyric acid (Wishart et al., 2018). As a crucial short-chain fatty acid (SCFA), butyrate is the product of microbial fermentation of undigested carbohydrates by *Clostridia*, *Eubacterium* and *Fusobacterium*. Recently, it was reported that the

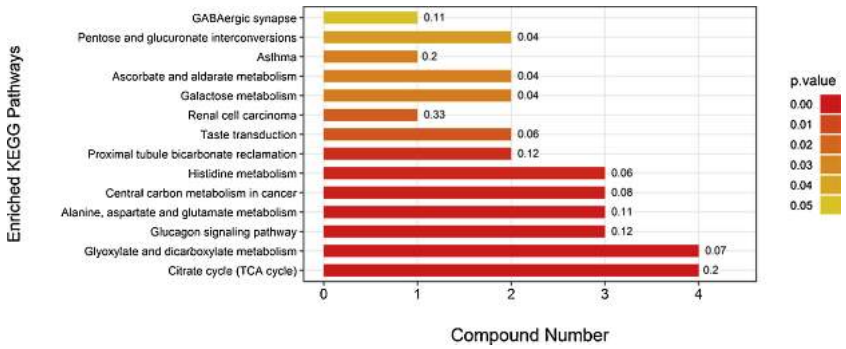

Fig. 5. Enriched KEGG pathway analysis for ST vs T2DM.

increase in gut production of the SCFA butyrate was associated with improved insulin response in T2DM patients (Sanna et al., 2019). Interestingly, our former studies showed that ST improved the inflammatory status and regulated the intestinal flora disorder of T2DM rats (Liu et al., 2018). Gut microbiota, such as *Clostridia* and *Firmicutes,* could be increased after treated with ST, which consistent with the results of this study. In summary, ST could modulate the imbalance of intestinal flora, such as *Clostridia,* then increase the generation of SCFA butyrate and HMPP, which reduce insulin resistance and antioxidant stress of T2DM.

The result of our previous study supported the use of ST as a potential treatment for improving inflammation in T2D (Liu et al., 2018). In this study, Nicotinamide *N*-oxide (FC = 3.06) in the urine of the ST group was significantly increased compared to those of the T2DM group. Nicotinamide *N*-oxide is a metabolite of nicotinamide having anti-inflammatory activity, and it increases with increasing concentration of nicotinamide (Szafarz, Lomnicka, Sternak, Chlopicki, & Szymura-Oleksiak, 2010). Besides, a higher level of nicotinamide could reduce LDL in blood (Zhang, Kamanna, Zhang, & Kashyap, 2008), which consist with the result that serum LDL and TG were significantly decreased after 4 weeks of ST treatment. In addition, nicotinamide is a major form of niacin and exerts physiological functions as a precursor of nicotinamide adenine dinucleotide (NAD + /NADH) and nicotinamide adenine dinucleotide phosphate (NADP + /NADPH) (Magni et al., 2004; Rongvaux, Andris, & Leo, 2010), which act mainly as a hydrogen donor in biosynthetic reactions, the synthesis of fatty acids and steroids for example. Therefore, nicotinamide plays an important role in the metabolism of carbohydrates, lipids and proteins. And the dysregulation of nicotinamide may be related to the development of several metabolic diseases including insulin resistance and type 2 diabetes (Imai, 2009).

Histamine is an organic nitrogenous compound involved in the inflammatory response through four receptors ($H_{1\text{-}4}R$), as well as regulating physiological functions in the gut (Nieto-Alamilla, Marquez-Gomez, Garcia-Galvez, Morales-Figueroa, & Arias-Montano, 2016; Pini, Obara, Battell, Chazot, & Rosa, 2016). Histamine intolerance is directly implicated in diabetes. Studies have consistently shown increased histamine levels in diabetics. Also, H_3R can be found in the pancreatic cells that secrete insulin. A major product of histamine metabolism, 1-methylhistamine, is generated along within mast cell activation. Previous studies suggested that advanced glycation end products that become overladen with glucose in diabetics, directly leading to mast-cell degranulation, which then releases histamine, moreover, mast-cell stabilizers and antihistamines have been shown to decrease complications from diabetes (Brown, Ind, Causon, & Lee, 1982; Shalit et al., 1988). Our study showed that levels of histamine and 1-methylhistamine in urine were substantially decreased (FC = 0.56 and 0.61) in ST treated group compared to those in T2DM group, which may reduce the possibility of stimulating inflammatory factors and improve the development of T2DM.

4. Conclusion

In conclusion, UPLC-ESI-Q-TOF-MS-based urinary metabolomics profiling and multivariate statistical analysis have been developed to evaluate the anti-diabetes effects of ST on HFD and low-dose STZ-induced T2DM rats. The results of biochemical parameters demonstrated the improved effects of ST treatment against T2DM. With OPLS-DA analysis, a clear separation between ST and T2DM group were achieved. Additionally, a total of 21 differential metabolites were identified in urinary samples, which help to explain the mechanisms of ST against T2DM. These metabolites were mainly associated with TCA cycle, carbohydrate metabolism and amino acid metabolism. After further analysis combined with previous studies, ST treatment partly exerted the anti-diabetes activity through regulating energy metabolism, gut microbiota changes and inflammation. Thus, the metabolomics approach was proved to be a promising tool in exploring the anti-diabetes effects of ST and provided a better understanding of the mechanisms of action.

Declaration of Competing Interest

The authors declare no conflict of interest.

Acknowledgement

This project was supported by the opening fund of Beijing Advanced Innovation Center for Food Nutrition and Human Health.

References

Azam, A. A., Pariyani, R., Ismail, I. S., Ismail, A., Khatib, A., Abas, F., ... Shaari, K. (2017). Urinary metabolomics study on the protective role ofOrthosiphon stamineusin Streptozotocin induced diabetes mellitus in rats via1H NMR spectroscopy. *BMC Complementary and Alternative Medicine, 17*(1), 278.

Brown, M. J., Ind, P. W., Causon, R., & Lee, T. H. (1982). A novel double-isotope technique for the enzymatic assay of plasma histamine: application to estimation of mast cell activation assessed by antigen challenge in asthmatics. *Journal of Allergy and Clinical Immunology, 69*(1), 20–24.

Dong, Y., Chen, Y. T., Yang, Y. X., Shou, D., & Li, C. Y. (2016). Urinary metabolomic profiling in zucker diabetic fatty rats with type 2 diabetes mellitus treated with glimepiride, metformin, and their combination. *Molecules, 21*(12), 1446.

Dunn, W. B., & Ellis, D. I. (2005). Metabolomics: Current analytical platforms and methodologies. *Trends in Analytical Chemistry, 24*(4), 285–294.

Faber, J. H., Malmodin, D., Toft, H., Maher, A. D., Crockford, D., Holmes, E., ... Baunsgaard, D. (2007). Metabonomics in diabetes research. *Journal of Diabetes Science and Technology, 1*(4), 549–557.

Guasch-Ferré, M., Hruby, A., Toledo, E., Clish, C. B., Martínez-González, M. A., Salas-Salvadó, J., ... Hu, F. B. (2016). Metabolomics in prediabetes and diabetes: A systematic review and meta-analysis. *Diabetes Care, 39*(5), 833.

Hold, G. L., Schwiertz, A., Aminov, R. I., Blaut, M., & Flint, H. J. (2003). Oligonucleotide probes that detect quantitatively significant groups of butyrate-producing Bacteria in human feces. *Applied and Environmental Microbiology, 69*(7), 4320–4324.

Imai, S. (2009). The NAD World: A new systemic regulatory network for metabolism and aging–Sirt1, systemic NAD biosynthesis, and their importance. *Cell Biochemistry and Biophysics, 53*(2), 65.

Larsen, N., Vogensen, F. K., Berg, F. W. J..., Nielsen, D. S., Andreasen, A. S., Pedersen, B. K., ... Jakobsen, M. (2010). Gut Microbiota in Human Adults with Type 2 Diabetes

Differs from Non-Diabetic Adults. *PloS One, 5*(2), e9085.
Liu, F., Gan, P. P., Wu, H., Wei, S. W., Ong, E. S., & Li, S. F. Y. (2012). A combination of metabolomics and metallomics studies of urine and serum from hypercholesterolaemic rats after berberine injection. *Analytical and Bioanalytical Chemistry, 403*(3), 847–856.
Liu, G., Bei, J., Liang, L., Yu, G., Li, L., & Li, Q. (2018). Stachyose improves inflammation through modulating gut microbiota of high-fat diet/streptozotocin induced type 2 diabetes in rats. *Molecular Nutrition & Food Research, 62*(6), 1700954.
Magni, G., Amici, A., Emanuelli, M., Orsomando, G., Raffaelli, N., & Ruggieri, S. (2004). Enzymology of NAD+ homeostasis in man. *Cellular and Molecular Life Sciences, 61*(1), 19–34.
Mayyas, F., Alzoubi, K. H., & Bonyan, R. (2016). The role of spironolactone on myocardial oxidative stress in rat model of streptozotocin-induced diabetes. *Cardiovascular Therapeutics, 35*(2), e12242.
Napolitano, A., Miller, S., Nicholls, A. W., Baker, D., Horn, S. V., Thomas, E., ... Nunez, D. J. (2014). Novel gut-based pharmacology of metformin in patients with type 2 diabetes mellitus. *PloS One, 9*(7), e100778.
Neth, K., Lucio, M., Walker, A., Zorn, J., Schmitt-Kopplin, P., & Michalke, B. (2015). Changes in brain Metallome/Metabolome pattern due to a single i.v. Injection of manganese in rats. *PloS One, 10*(9), e0138270.
Nicholson, J. K., Lindon, J. C., & Holmes, E. (1999). "Metabonomics": Understanding the metabolic responses of living systems to pathophysiological stimuli via multivariate statistical analysis of biological NMR spectroscopic data. *Xenobiotica, 29*(11), 1181–1189.
Nieto-Alamilla, G., Marquez-Gomez, R., Garcia-Galvez, A. M., Morales-Figueroa, G. E., & Arias-Montano, J. A. (2016). The histamine H3 receptor: Structure, pharmacology and function. *Molecular Pharmacology, 90*(5), 649.
Oexle, H., Gnaiger, E., & Weiss, G. (1999). Iron-dependent changes in cellular energy metabolism: Influence on citric acid cycle and oxidative phosphorylation. *Biochimica et Biophysica Acta, 1413*(3), 99–107.
Pini, A., Obara, I., Battell, E., Chazot, P. L., & Rosa, A. C. (2016). Histamine in diabetes: is it time to reconsider? *Pharmacological Research, 111*, 316–324.
Poovitha, S., Sai, M. S., & Parani, M. (2017). Protein extract from the fruit pulp of Momordica dioica shows anti-diabetic, anti-lipidemic and antioxidant activity in diabetic rats. *Journal of Functional Foods, 33*, 181–187.
Rongvaux, A., Andris, F., & Leo, O. (2010). Reconstructing eukaryotic NAD metabolism. *Bioessays, 25*(7), 683–690.
Sanna, S., van Zuydam, N. R., Mahajan, A., Kurilshikov, A., Vich Vila, A., Võsa, U., ... McCarthy, M. I. (2019). Causal relationships among the gut microbiome, short-chain fatty acids and metabolic diseases. *Nature Genetics, 51*, 600–605.
Schwarz, P. E. H., Gallein, G., Ebermann, D., Müller, A., Lindner, A., Rothe, U., ... Müller, G. (2013). Global Diabetes Survey—An annual report on quality of diabetes care. *Diabetes Research and Clinical Practice, 100*(1), 11–18.
Shalit, M., Schwartz, L. B., Golzar, N., Vonallman, C., Valenzano, M., Fleekop, P., ... Zweiman, B. (1988). Release of histamine and tryptase in vivo after prolonged cutaneous challenge with allergen in humans. *The Journal of Immunology, 141*(3), 821.
Shin, N. R., Lee, J. C., Lee, H. Y., Kim, M. S., Whon, T. W., Lee, M. S., ... Bae, J. W. (2014). An increase in the Akkermansia spp. Population induced by metformin treatment improves glucose homeostasis in diet-induced obese mice. *Gut, 63*(5), 727–735.
Smith, C. A., Want, E. J., O'Maille, G., Abagyan, R., & Siuzdak, G. (2006). XCMS: Processing mass spectrometry data for metabolite profiling using nonlinear peak alignment, matching, and identification. *Analytical Chemistry, 78*(3), 779–787.
Szafarz, M., Lomnicka, M., Sternak, M., Chlopicki, S., & Szymura-Oleksiak, J. (2010). Simultaneous determination of nicotinic acid and its four metabolites in rat plasma using high performance liquid chromatography with tandem mass spectrometric detection (LC/MS/MS). *Journal of Chromatography B, 878*(11), 895–902.
Wang, X., Zhang, A., Han, Y., Wang, P., Sun, H., Song, G., ... Zhang, M. (2012). Urine metabolomics analysis for biomarker discovery and detection of jaundice syndrome in patients with liver disease. *Molecular & Cellular Proteomics, 11*(8), 370.
Wild, S., Roglic, G., Green, A., Sicree, R., & King, H. (2004). Global prevalence of diabetes: Estimates for the year 2000 and projections for 2030. *Diabetes Care, 24*, 1047–1053.
Wishart, D. S., Feunang, Y. D., Marcu, A., Guo, A. C., Liang, K., Vázquez-Fresno, R., ... Scalbert, A. (2018). HMDB 4.0: The human metabolome database for 2018. *Nucleic Acids Research, 46*, D608–D617.
Yin, J., Yang, G., Wang, S., & Chen, Y. (2006). Purification and determination of stachyose in Chinese artichoke (Stachys sieboldii Miq.) by high-performance liquid chromatography with evaporative light scattering detection. *Talanta, 70*(1), 208–212.
Zhang, L. H., Kamanna, V. S., Zhang, M. C., & Kashyap, M. L. (2008). Niacin inhibits surface expression of ATP synthase beta chain in HepG2 cells: Implications for raising HDL. *Journal of Lipid Research, 49*(6), 1195–1201.
Zhang, R. X., Jia, Z. P., Kong, L. Y., Ma, H. P., Ren, J., Li, M. X., ... Ge, X. (2004). Stachyose extract from Rehmannia glutinosa Libosch. To lower plasma glucose in normal and diabetic rats by oral administration. *Die Pharmazie, 59*(7), 552.
Zhang, S., Xu, H., Yu, X., Yi, W., & Sui, D. (2017). Metformin ameliorates diabetic nephropathy in a rat model of low-dose streptozotocin-induced diabetes. *Experimental and Therapeutic Medicine, 14*(1), 383.